MASTER COPY KEEP THIS COPY FOR REPRODUCTION PURPOSES

AD-A266 711

ATION PAGE

Form Approved
OMB No. 0704-0188

1. AGENCY USE ONLY (Leave ...)	DATE	3. REPORT TYPE AND DATES COVERED
		Reprint

4. TITLE AND SUBTITLE

Title shown on Reprint

5. FUNDING NUMBERS

2

DAAL03-91-C-0025

6. AUTHOR(S)

Author(s) listed on Reprint

7. PERFORMING ORGANIZATION NAME(S) AND ADDRESS(ES)

Rockwell International Corp.
Canoga Park, California 91309

8. PERFORMING ORGANIZATION REPORT NUMBER

9. SPONSORING / MONITORING AGENCY NAME(S) AND ADDRESS(ES)

U. S. Army Research Office
P. O. Box 12211
Research Triangle Park, NC 27709-2211

10. SPONSORING / MONITORING AGENCY REPORT NUMBER

ARO 28655.10-CH

11. SUPPLEMENTARY NOTES

The view, opinions and/or findings contained in this report are those of the author(s) and should not be construed as an official Department of the Army position, policy, or decision, unless so designated by other documentation.

12a. DISTRIBUTION / AVAILABILITY STATEMENT

Approved for public release; distribution unlimited.

12b. DISTRIBUTION CODE

13. ABSTRACT *(Maximum 200 words)*

ABSTRACT ON REPRINT

14. SUBJECT TERMS			15. NUMBER OF PAGES
			16. PRICE CODE
17. SECURITY CLASSIFICATION OF REPORT	18. SECURITY CLASSIFICATION OF THIS PAGE	19. SECURITY CLASSIFICATION OF ABSTRACT	20. LIMITATION OF ABSTRACT
UNCLASSIFIED	UNCLASSIFIED	UNCLASSIFIED	UL

DISCLAIMER NOTICE

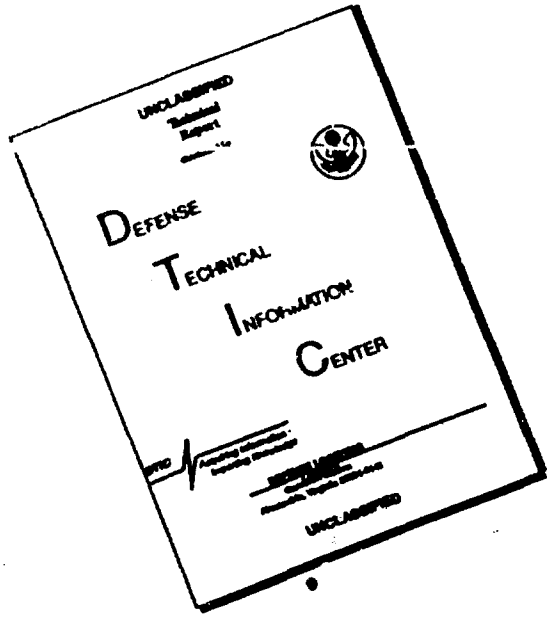

THIS DOCUMENT IS BEST QUALITY AVAILABLE. THE COPY FURNISHED TO DTIC CONTAINED A SIGNIFICANT NUMBER OF PAGES WHICH DO NOT REPRODUCE LEGIBLY.

Reprinted from the Journal of the American Chemical Society, 1993, 115.

The IOF_6^- Anion: The First Example of a Pentagonal Bipyramidal AX_5YZ Species†

K. O. Christe,*[1] D. A. Dixon,[2] A. R. Mahjoub,[3] H. P. A. Mercier,[4] J. C. P. Sanders,[4] K. Seppelt,*[3] G. J. Schrobilgen,*[4] and W. W. Wilson[1]

Contribution from Rocketdyne, A Division of Rockwell International, Canoga Park, California 91309, the Department of Chemistry, McMaster University, Hamilton, Ontario L8S 4M1, Canada, the Central Research and Development Department, E.I. du Pont de Nemours and Company, Inc., Experimental Station, Wilmington, Delaware 19880-0328, and the Institut für Anorganische und Analytische Chemie der Freien Universität, Berlin, Germany

Received October 16, 1992

Abstract: The IOF_6^- anion, which is the first example of a pentagonal bipyramidal AX_5YZ type species, was prepared in the form of its stable $N(CH_3)_4^+$ salt. Its X-ray crystal structure was determined at −93 ° and −155 °C (tetragonal, space group $P4/nmm$, $Z = 2$, $a = 8.8590$ (10) and 8.8151 (10) Å, $c = 6.3690$ (10) and 6.3213 (10) Å, $R = 0.0373$ and 0.0291 for 876 [$I > 3\sigma(I)$] and 885 [$I > 3\sigma(I)$] reflections, respectively). In addition to two perfectly ordered $N(CH_3)_4^+$ cations, the structure contains two IOF_6^- anions of approximate C_{5v} symmetry which are subject to a positional 4-fold disorder for the equatorial plane. The O–I–F_{ax} angle is constrained by symmetry to be 180°, whereas there are no constraints on the positions of the equatorial fluorines. The I–O bond length indicates substantial double bond character, and the axial I–F bond length is significantly shorter than the five equatorial I–F bond lengths. The mean O–I–F_{eq} bond angle is slightly larger than 90°, due to the doubly bonded oxygen atom being more repulsive than the singly bonded axial fluorine ligand. The equatorial IF_5 plane is puckered to alleviate its congestion. In contrast to the highly fluxional, free IF_7 molecule, in which the equatorial fluorines undergo a very rapid, dynamic, pseudorotational ring puckering and a slower intramolecular equatorial–axial ligand exchange, the puckering of the IOF_6^- anion in its $N(CH_3)_4^+$ salt is frozen out due to anion–cation interactions, and the equatorial–axial ligand exchange is precluded by the more repulsive oxygen ligand which occupies exclusively axial positions. Therefore, the IOF_6^- anion is ideally suited for studying the nature of the equatorial puckering in species of 5-fold symmetry. The puckering in IOF_6^- is of the C_s symmetry type, and the deviations from the ideal equatorial plane are relatively small and decrease with decreasing temperature. Furthermore, the axial I–O bond length decreases and the mean O–I–F_{eq} bond angle increases with decreasing temperature. These findings demonstrate that in agreement with our results from ab initio calculations and contrary to the VSEPR concept of repelling points on a sphere, the minimum energy structures of these main group heptacoordinated fluorides or oxyfluorides are those of pentagonal bipyramids with an unpuckered equatorial plane and not those of either monocapped octahedra or monocapped trigonal prisms. Whereas in solid $N(CH_3)_4^+IOF_6^-$ the equatorial ring puckering of IOF_6^- is frozen out, in the dissolved free ion this puckering becomes dynamic, as demonstrated by ^{19}F NMR spectroscopy which shows five equivalent equatorial fluorine ligands. Contrary to IF_7 and TeF_7^-, the IOF_6^- anion does not undergo an intramolecular equatorial–axial ligand exchange on the NMR time scale because of the more repulsive, doubly bonded oxygen. The vibrational spectra of $N(CH_3)_4^+IOF_6^-$ in both the solid state and CH_3CN solution were recorded and assigned with the help of ab initio calculations on IOF_6^- using effective core potentials and local density functional theory. Normal coordinate analyses were carried out for the pentagonal bipyramidal series IF_7, IOF_6^-, XeF_5^- which show that the equatorial, in-plane deformation force constants (f_α) are a good measure for the degree of congestion in the equatorial plane. Puckering increases with decreasing bond lengths, increasing ligand and decreasing central atom sizes, and increasing temperature. The pentagonal bipyramidal structures of these molecules and the coplanarity of their equatorial ligands, which are found for their minimum energy structures, are explained by a bonding scheme involving delocalized p_{xy} hybrid orbitals of the central atom for the formation of a coplanar, semi-ionic, 6-center 10-electron bond system for the five equatorial bonds and of an sp_z hybrid orbital for the formation of two, more covalent, colinear, axial bonds. This bonding scheme can account for all the observed structural features and also the bond length differences.

Introduction

In main group element chemistry, coordination numbers in excess of six are relatively rare, but they are of considerable interest due to special features caused by steric crowding of the ligands, free valence electron pairs being sterically either active or inactive, and the propensity of the molecules to exhibit fluxionality. Of particular interest are heptacoordinated species which could exist either as a monocapped octahedron, a monocapped trigonal prism, or a pentagonal bipyramid.[5] According to the VSEPR model of "repelling points on a sphere",[5] the preferred structures should be the monocapped octahedron or trigonal prism. However, for main group elements and relatively low repulsive forces, the pentagonal bipyramid is favored[6] and has been found for species such as IF_7[7,8] or TeF_7^-.[9-11] In pentagonal bipyramidal structures, the pentagonal equatorial plane is highly congested which results in increased repulsion

† Dedicated to Professor Jean'ne Shreeve on the occasion of her 60th birthday.

(1) Rockwell International, Rocketdyne Division.
(2) E.I. du Pont de Nemours and Company, Inc.
(3) Freie Universität, Berlin.
(4) McMaster University.

(5) Gillespie, R. J.; Hargittai, I. In *The VSEPR Model of Molecular Geometry*; Allyn and Bacon, A Division of Simon & Schuster, Inc.: Needham Heights, MA, 1991; p 58.
(6) Thompson, H. B.; Bartell, L. S. *Inorg. Chem.* **1968**, *7*, 488.
(7) Adams, W. J.; Thompson, H. B.; Bartell, L. S. *J. Chem. Phys.* **1970**, *53*, 4040.

0002-7863/93/1515-2696$04.00/0

among the equatorial ligands and, as a result, in increased bond lengths and usually some kind of puckering.[5-8] In the case of 5-fold symmetry, this puckering presents a special problem. The odd number of ligands does not allow for a highly symmetric arrangement in which all five equatorial ligands can be placed into equivalent positions, i.e. with identical displacements alternately above and below the equatorial plane. One way to achieve equivalency of the equatorial ligands is a fast, dynamic, pseudorotational ring puckering, as found for IF_7,[7,8] which results in a highly fluxional molecule. In addition, the pentagonal bipyramidal XF_7 molecules generally exhibit a second kind of fluxionality, i.e. a slower, intramolecular, axial–equatorial ligand exchange.[8] The combination of these two types of fluxionality makes it experimentally very difficult to characterize and describe the structures of these molecules. Many of the difficulties with the fluxionality of the XF_7 species might be overcome by studying ionic XOF_6^{n-} salts. The presence of one doubly bonded oxygen which is more repulsive than the fluorine ligands should preempt a facile axial–equatorial ligand exchange, and the dynamic puckering of the equatorial plane could be frozen out by anion–cation interactions. Therefore, an effort was undertaken to prepare and characterize a salt containing an XOF_6^- anion. Examples of pentagonal bipyramidal XOF_6 species had previously been unknown and only recently been reported[10,11] in two separate preliminary notes from our laboratories. In this paper, a full account and analysis of our work on the IOF_6^- anion is given.

Experimental Section

Caution: IOF_5 is a strong oxidizer, and its combination with organic materials, such as CH_3CN or $N(CH_3)_4^+$ salts, could be potentially hazardous. Although no difficulties were encountered in the present study, appropriate safety precautions and shielding should be used, particularly when working on a larger scale with these materials.

Materials. The CH_3CN (Baker, Bio-analyzed, having a water content of 40 ppm) was treated with P_2O_5 and freshly distilled prior to use, thereby reducing its water content to <4 ppm. Literature methods were used for the syntheses of IOF_5[12-14] and anhydrous $N(CH_3)_4^+F^-$.[15]

Synthesis of $N(CH_3)_4^+IOF_6^-$. The salt $N(CH_3)_4^+IOF_6^-$ was prepared by condensing gaseous IOF_5 (6.40 mmol) from the calibrated volume of a nickel and stainless steel vacuum line at room temperature onto anhydrous $N(CH_3)_4^+F^-$ (0.4473 g, 5.779 mmol) in 8 mL of dry CH_3CN at −196 °C. The mixture was warmed and allowed to react, with frequent agitation, at −35 °C for 30 min. The solvent and unreacted IOF_5 were pumped off at −35 °C leaving behind $N(CH_3)_4^+IOF_6^-$ as a very pale yellow crystalline solid in essentially quantitative yield (1.8298 g, 5.772 mmol). Anal. Calcd for $C_4H_{12}F_6IO$: C, 14.50; H, 3.63; F, 33.00; I, 38.35; N, 4.23. Found: C, 14.62; H, 3.66; F, 32.4; I, 38.51; N, 4.33.

Vibrational Spectroscopy. Raman spectra were recorded on either a Cary Model 83 or a Spex Model 1403 spectrophotometer using the 488-nm exciting line of an Ar ion or the 647.1-nm line of a Kr ion laser, respectively. Baked-out Pyrex melting point capillaries or thin-walled Kel-F tubes were used as sample containers. A previously described[16] device was used for recording the low-temperature spectra.

Infrared spectra were recorded by using either AgCl or AgBr disks on a Perkin-Elmer Model 283 spectrophotometer. The finely powdered samples were sandwiched between two thin disks and pressed together in a Wilks minipress inside the drybox.

Nuclear Magnetic Resonance Spectroscopy. The ^{19}F NMR spectra were recorded at McMaster University unlocked (field drift < 0.1 Hz h^{-1}) on a Bruker AM-500 spectrometer equipped with an 11.744 T cryomagnet and an Aspect 3000 computer. The spectra were obtained using a 5-mm combination $^1H/^{19}F$ probe operating at 470.599 MHz. The spectra were recorded in a 32K memory. A spectral width setting of 62 500 Hz was employed, yielding a data point resolution of 3.8 Hz/data point and an acquisition time of 0.262 s. No relaxation delays were applied. Typically, 40 000 transients were accumulated. The pulse width corresponding to a bulk magnetization tip angle, θ, of approximately 90° was equal to 1 μs. Line broadening parameters used in the exponential multiplication of the free induction decays were 3–4 Hz.

The low-temperature study was carried out by the use of a Bruker temperature controller. The temperature was measured with a copper–constantan thermocouple inserted directly into the sample region of the probe and was accurate to ±1 °C.

The spectra were referenced to a neat external sample of $CFCl_3$. The chemical shift convention used is that a positive (negative) sign signifies a chemical shift to high (low) frequency of the reference compound.[17]

Computational Methods. The electronic structure calculations were done at the ab initio molecular orbital level using either local density function (LDF) theory[18-21] or effective core potentials (ECP). The LDF calculations were carried out with the program system DMol,[22] as previously described,[8] with a double-numerical basis set augmented by d polarization functions. This can be considered in terms of size as a polarized double-ζ basis set. However, because exact numerical solutions are employed for the atom, this basis set is of significantly higher quality than a normal molecular orbital polarized double-ζ basis set. The fitting functions have an angular momentum number one greater than that of the polarization function, resulting in a value of $l = 3$ for the fitting functions.

The ECP calculations were done with all electrons on the F and O and with an effective core potential replacing all of the *core electrons* on the I. The valence basis set is of polarized double-ζ quality. The fluorine and oxygen basis set is from Dunning and Hay,[23] and the ECP from Hay and Wadt[24] including relativistic corrections. The valence basis set of Hay and Wadt[24] was used augmented by a d function on I with an exponent of 0.266.[25] The geometries were optimized by using gradient techniques,[26] and the force fields were calculated analytically.[27,28] The ab initio MO calculations were done with the program GRADSCF,[29] as implemented on a Cray YMP computer system.

Crystal Structure Determinations of $N(CH_3)_4^+IOF_6^-$. Two independent crystal structure determinations were carried out for this compound at McMaster University and the Freie Universität Berlin.

(8) Christe, K. O.; Curtis, E. C.; Dixon, D. A. *J. Am. Chem. Soc.* **1993**, *115*, 1520.
(9) Selig, H.; Sarig, S.; Abramowitz, S. *Inorg. Chem* **1974**, *13*, 1508.
(10) Christe, K. O.; Sanders, J. C. P.; Schrobilgen, G. J.; Wilson, W. W. *J. Chem. Soc., Chem. Commun.* **1991**, 837.
(11) Mahjoub, A. R.; Seppelt, K. *J. Chem. Soc., Chem. Commun.* **1991**, 840.
(12) Holloway, J. H.; Selig, H.; Claassen, H. H. *J. Chem. Phys.* **1971**, *54*, 4305.
(13) Schack, C. J.; Pilipovich, D.; Cohz, S. N.; Sheehan, D. F. *J. Phys Chem.* **1968**, *72*, 4697.
(14) Schack, C. J.; Christe, K. O. *J. Fluorine Chem.* **1990**, *49*, 167.
(15) Christe, K. O.; Wilson, W. W.; Wilson, R. D.; Bau, R.; Feng, J. *J. Am. Chem. Soc.* **1990**, *112*, 7619.
(16) Miller, F. A.; Harney, B. M. *Appl. Spectrosc.* **1969**, *23*, 8.
(17) *Pure Appl. Chem.* **1972**, *29*, 627; **1976**, *45*, 217.
(18) Parr, R. G.; Yang, W. *Density Functional Theory of Atoms and Molecules*; Oxford University Press: New York, 1989.
(19) Salahub, D. R. In *Ab Initio Methods in Quantum Methods in Quantum Chemistry*, 2nd ed.; Lawley, K. P., Ed.; J. Wiley & Sons: New York, 1987; p 447.
(20) (a) Wimmer, E.; Freeman, A. J.; Fu, C.-L.; Cao, P.-L.; Chou, S.-H.; Delley, B. In *Supercomputer Research in Chemistry and Chemical Engineering*; Jensen, K. F., Truhlar, D. G., Eds.; ACS Symp. Ser.; American Chemical Society: Washington, DC, 1987; p 49. (b) Dixon, D. A.; Andzelm, J.; Fitzgerald, G.; Wimmer, E.; Delley, B. In *Science and Engineering on Cray Supercomputers. Proceedings of the Fifth International Symposium*; Cray Research: Minneapolis, MN, 1990; p 285.
(21) Jones, R. O.; Gunnarsson, O. *Rev. Mod. Phys.* **1989**, *61*, 689.
(22) Delley, B. *J. Chem. Phys.* **1990**, *92*, 508. DMol is available commercially from BIOSYM Technologies, San Diego, CA.
(23) Dunning, T. H., Jr.; Hay, P. J. In *Methods of Electronic Structure Theory*; Schaefer, H. F., III, Ed.; Plenum Press: New York, 1977; Chapter 1.
(24) Hay, P. J.; Wadt, W. R. *J. Chem. Phys.* **1985**, *82*, 299.
(25) Huzinaga, S.; Andzelm, J.; Klobukowski, M.; Radzio, E.; Sakai, Y.; Tatasaki, H. *Gaussian Basis Sets of Molecular Calculations*; Elsevier: Amsterdam, 1984.
(26) (a) Kormonicki, A.; Ishida, K.; Morokuma, K.; Ditchfield, R.; Conrad, M. *Chem. Phys. Lett.* **1977**, *45*, 595. (b) McIver, J. W., Jr.; Komornicki, A. *Chem. Phys. Lett.* **1971**, *10*, 202. (c) Pulay, P. In *Applications of Electronic Structure Theory*; Schaefer, H. F., III, Ed.; Plenum Press: New York, 1977; p 153.
(27) (a) King, H. F.; Komornicki, A. *J. Chem. Phys.* **1986**, *84*, 5465. (b) King, H. F.; Komornicki, A. In *Geometrical Derivatives of Energy Surfaces and Molecular Properties*; Jorgenson, P., Simons, J., Eds.; NATO ASI Series C; D. Reidel: Dordrecht, 1986; Vol. 166, p 207.
(28) Breidung, J.; Thiel, W.; Komornicki, A. *Chem. Phys. Lett.* **1988**, *153*, 76.
(29) GRADSCF is an ab initio program system designed and written by A. Komornicki at Polyatomics Research.

At McMaster, only one type of crystal was observed, tetragonal *P4/nmm* crystals which have IOF_6^- with a positional 4-fold disorder for the puckered equatorial plane. The structure of one of these crystals was determined at −93 °C and is given in this paper.

At Berlin, originally a very similar, orthorhombic crystal was studied at −163 °C, and the data were refined either in *P4/nmm* with 4-fold disorder or *Pmmn* with systematic twinning; however, no puckering of the equatorial plane was observed.[11] In repeat experiments, exclusively crystals identical to those found at McMaster were obtained. The structure of one of these crystals was determined at −155 °C and is given in this paper.

Single crystals of $N(CH_3)_4^+IOF_6^-$ were grown at McMaster by making a saturated solution of $N(CH_3)_4^+IOF_6^-$ in CH_3CN in a Teflon-FEP tube at room temperature and warming it to 45 °C whereupon it completely dissolved to give a pale yellow solution. The sample tube was then positioned horizontally above a dewar containing water at 60 °C, covered with aluminum foil, and slowly allowed to cool overnight. This resulted in the growth of transparent crystals which could be described as tetragonal prisms. At McMaster, the crystals were sealed in Lindemann quartz capillaries and centered on a Siemens R3m/v diffractometer. Accurate cell dimensions were determined at $T = -93$ °C from a least-squares refinement of the setting angles (χ, ϕ, and 2θ) obtained from 25 accurately centered reflections (with $34.71° \le 2\theta \le 38.05°$) chosen from a variety of points in reciprocal space. Examination of the peak profiles revealed that they were single.[30] Integrated diffraction intensities were collected using a θ–2θ scan technique with scan rates varying from 1.5 to 14.65°/min (in 2θ) and a scan range of ±0.6°, so that the weaker reflections were examined slowly to minimize counting errors. Data were collected in four steps since the crystal was diffracting very strongly. In the first step, the data were collected with $-15 \le h \le 15$, $0 \le k \le 15$, and $0 \le l \le 11$ and with $3° \le 2\theta \le 45°$, using silver radiation monochromatized with a graphite crystal ($\lambda = 0.56087$ Å). During data collection, the intensities of three standard reflections were monitored every 97 reflections to check for crystal stability and alignment. A total of 1583 reflections were collected out of which 16 were standard reflections. At this stage, the distribution of the reflections in the reciprocal space indicated that the crystal was diffracting at relatively high angles, consequently a second data set was recorded with $45° \le 2\theta \le 55°$. This time a total of 1163 reflections were collected out of which 12 were standard reflections. Finally, a third data set was recorded with $55° \le 2\theta \le 60°$ giving rise to 712 reflections out of which 8 were standard reflections. These data sets were recorded with the maximum intensity (i.e. 1.5 kW Ag X-rays), without attenuation, and as a consequence, the strongest reflections at very low angles were not recorded. In order to record these missing reflections, the power had to be decreased to 750 W. Another set of data was collected with $-3 \le h \le 3$, $0 \le k \le 3$, and $0 \le l \le 2$. A total of 31 reflections were collected, out of which 6 were standard reflections. No crystal decay was observed. In total, 3136 reflections were collected and 876 unique reflections remained after averaging of equivalent reflections. A total of 780 reflections, satisfying the condition $I \ge 3\sigma(I)$, were used for the structure solution. These reflections exhibited systematic absences for *hk*0: $h + k = 2n$ and *h*00: $h = 2n$. Corrections were made for Lorentz and polarization effects. Absorption corrections were applied by using the program DIFABS.[31] The transmission factors ranged from 0.728 to 1.117.

The XPREP program[32] was used to determine the correct cell and space group. It confirmed that the original cell was correct and that the lattice was tetragonal primitive ($R_{int} = 0.028$). The structure was shown to be centrosymmetric by an examination of the *E*-statistics (calculated, 0.616; theoretical, 0.736). The two space groups which were consistent with the systematic absences (*n*-glide and C_2) were the centrosymmetric *P4/n* and *P4/nmm* space groups.

A first solution was obtained without absorption corrections; it was achieved in the space group *P4/nmm* (129) by conventional heavy-atom Patterson methods which located the positions of the iodine, nitrogen, and carbon atoms on special positions (i.e. *4mm*, *−4m2*, *.m.*). The full-matrix least-squares refinement of their positions and isotropic thermal parameters gave a conventional agreement index $R = (\sum||F_o| - |F_c||/\sum|F_o|)$ of 0.12. A subsequent difference Fourier synthesis revealed the positions of two atoms located on special positions, above and below the iodine. It was possible to distinguish a fluorine from an oxygen atom from the difference in bond lengths (i.e., 1.83 and 1.74 Å). The introduction of these positions gave a residual factor *R* of 0.10. A further difference Fourier synthesis clearly showed the presence of three atoms in the equatorial environment of the iodine. Two of these atoms were positioned on general positions, while the third one was positioned on a special position (*..m*). Consequently, the model implied a 4-fold disorder in the "pseudo"-equatorial plane consisting of a superposition of four molecules with *identical I, axial F, and O positions. Consequently, the site occupancy* factors of the equatorial fluorine atoms were set equal to 0.25 and 0.125 (general and special positions, respectively) instead of 1.00 and 0.5. The introduction of these positions and isotropic thermal parameters for the equatorial F atoms (all set equal) resulted in a drop of the residual factor *R* to 0.057. Another improvement of the structure was achieved by introducing anisotropic thermal parameters for the I, N, C, F_{ax}, and O atoms (the F_{eq} were kept isotropic because of the presence of the 4-fold disorder), and the positions of the hydrogen atoms located from a difference Fourier map (U(H) fixed to 0.08 Å^2), as well as a weighting factor ($w = 1/\sigma^2(F) - 0.0003F^2$), dropping the *R* factor to 0.044 ($R_w = 0.041$).

The structure was solved a second time using data that had been corrected for absorption. The initial model used the atomic coordinates and isotropic thermal parameters defined previously for all the atoms. The solution obtained ($R = 0.043$) indicated a slight improvement over that obtained without absorption corrections ($R = 0.057$). The final refinement was obtained by introducing anisotropic thermal parameters for the I, F_{ax}, O, N, and C atoms and a weighting factor ($w = 1/\sigma^2(F) + 0.0000F^2$) and gave rise to a residual *R* of 0.0373 ($R_w = 0.0350$). In the final difference Fourier map, the maximum and the minimum electron densities were 1.5 and −1.6 Å^3.

All calculations were performed using the SHELXTL PLUS[32] determination package for structure determination molecular graphics.

At Berlin, the crystal was mounted, with the help of a special apparatus,[33] on an Enraf Nonius CAD 4 diffractometer at −155 °C. Oscillating crystal photographs were used to check the reflection quality. There were 25 reflections in the ϑ range 12–25° that were used to obtain *the orientation matrix and lattice constants*. Space group determination: The lattice constants indicated no deviation from tetragonal symmetry. Reflection intensities obeyed the rules $F(hkl) = F(\bar{h}kl) = F(k\bar{h}l)$ with $R_{int} = 0.0204$. Extinction of $hk0 \neq 2n$ left only space group *P4/nmm* (No. 129), which enforces the 4-fold disorder model. Calculations in orthorhombic space groups *Pmmn* (No. 59) or $P2_1mn$ (No. 31) generated the same disorder of the equatorial fluorine atoms. Three reflections were used to check for crystal decay and standard reflections orientation. Further details of the measurement routine are given in Tables I and S1 (supplementary material). After applying Lorentz and polarization

Table I. Summary of Crystal Data and Refinement Results for $N(CH_3)_4^+IOF_6^-$ at −93 and −155 °C

T (°C)	−93	−155
space group	*P4/nmm* (tetragonal)	
a (Å)	8.8590(10)	8.8151(10)
c (Å)	6.3690(10)	6.3213(12)
V (Å^3)	499.85(11)	491.20(10)
molecules/unit cell	2	
molecular weight	331.0	
cryst dimens (mm)	0.4 × 0.5 × 0.2	0.4 × 0.4 × 0.4
calcd density (g cm^{-3})	2.199	2.238
color	very faintly yellow	
cryst decay (%)	no	no
abs coeff (mm^{-1})	3.259	3.326
wavelength (Å) used for data collection	0.56086	0.71069
sin θ/λ limit (Å^{-1})	0.8915	0.9045
total no. of reflctns measd	3136	3489
no. of independent reflctns	876	887
no. of reflctns used in structural analysis, $I > 3\sigma(I)$	780	885
no. of variable parameters	28	34
final agreement factors		
R	0.0373	0.0291
R_w	0.0350	0.0255

(30) Despite the fact that all the peaks proved to be single, the possibility of twinning was checked by verifying that the *hkl* values associated with the very weak and very strong reflections at low sin θ/λ refined using the same orientation matrix.

(31) Walker, N.; Stuart, D. *Acta Crystallogr.* **1983**, *A39*, 158.

(32) Sheldrick, G. M. (1990); SHELXTL PLUS™ Release 4.21/V. Siemens Analytical X-Ray Instruments, Inc., Madison, Wisconsin.

(33) Keith, M.; Bärnighausen, H. A. *Kristallogr.* **1985**, *170*, 5. Schumann, H.; Genthe, W.; Hahn, F.; Hossein, M. B.; d. Helin, D. V. *Organomet. Chem.* **1986**, *229*, 67.

Table II. Bond Lengths, Bond Angles, Average Equatorial Plane Angle, and Deviations from the Average O–I–F_{eq} Bond Angle for $N(CH_3)_4^+IOF_6^-$ at −93 and −155 °C

	bond lengths (Å)		deviations (deg) from the mean O–I–F_{eq} bond angle	
	−93 °C	−155 °C	−93 °C	−155 °C
I–O	1.772(8)	1.745(4)		
I–F(1)	1.822(6)	1.823(3)		
I–F(2)	1.899(9)	1.894(5)	−0.8(2)	−0.4(1)
I–F(3)	1.852(10)	1.868(7)	5.2(2)	3.7(2)
I–F(4)	1.880(14)	1.868(9)	−8.7(4)	−6.6(3)
N–C	1.483(4)	1.491(3)		

	bond angles (deg)	
	−93 °C	−155 °C
O–I–F(2)	94.3(2)	95.9(1)
O–I–F(3)	88.3(2)	91.8(2)
O–I–F(4)	102.4(4)	102.1(3)
F(1)–I–F(2)	85.7(2)	84.1(1)
F(1)–I–F(3)	91.7(2)	88.2(2)
F(1)–I–F(4)	77.8(4)	77.9(3)
F(3)–I–F(2e)	68.7(4)	69.9(3)
F(4)–I–F(3)	78.6(3)	76.1(2)
F(2c)–I–F(2e)	66.8(5)	67.5(3)
mean O–I–F_{eq}	93.5(3)	95.5(2)
mean pucker angle[a]	4.14(30)	2.96(20)

[a] Mean deviation of the equatorial fluorine ligands from the mean O–I–F_{eq} angle.

corrections, the data were used for refinement of the previously published[11] model with the program SHELXS 76.[34] Atomic form factors were taken from the Kynoch tables.[35] The atoms I, O, F(1), N, and C were refined anisotropically and F(2)–F(4) isotropically which resulted in $R = 0.045$. Absorption correction was introduced at this stage. Optical measurements were not possible because of the embedding of the colorless crystal in paraffin oil. The ψ scan method gave no better results. Finally the method DIFABS[31] was used. Maximal and minimal corrections of 1.28 and 0.85 were applied. At this stage, hydrogen atoms were found in difference Fourier maps and refined with fixed isotropic U. This model refined to $R = 0.0291$ and $R_w = 0.0255$ (see Table I). The 4-fold disordered atoms F(2)–F(4) were then treated anisotropically. This resulted in $R = 0.020$ and $R_w = 0.0171$. The F(2), F(3), and F(4) atoms became quite disk-like, with a considerable bond shrinkage effect. Since it is unclear whether or not it is advisable to refine these 4-fold disordered atoms anisotropically because of overlap of these atoms with each other, the calculations with isotropic F(2), F(3), F(4) atoms is regarded as the best solution.

Summaries of the data collection parameters and other crystallographic information for both data sets are given in Table I. The final atomic coordinates, thermal parameters, interatomic distances, bond angles, and deviations from the average O–I–F_{eq} angles are listed in Tables II and S4–S5 (supplementary material). Summaries of the structure determinations and the observed and calculated structure factors are given in Tables S1–S3.

Results and Discussion

Synthesis and Properties of $N(CH_3)_4^+IOF_6^-$. In a previous study,[36] it was shown that at room temperature, CsF does not react with a large excess of IOF_5, while at higher temperatures it tends to undergo deoxygenation. In the same paper it was speculated that the failure to observe fluorine–oxygen exchange in the IF_7–$CsNO_3$ system might be due to the lack of formation of an intermediate IOF_6^- salt. The present study clearly demonstrates that under suitable reaction conditions, i.e. using a soluble anhydrous fluoride of a large cation in a compatible solvent, IOF_6^- salts are readily formed according to

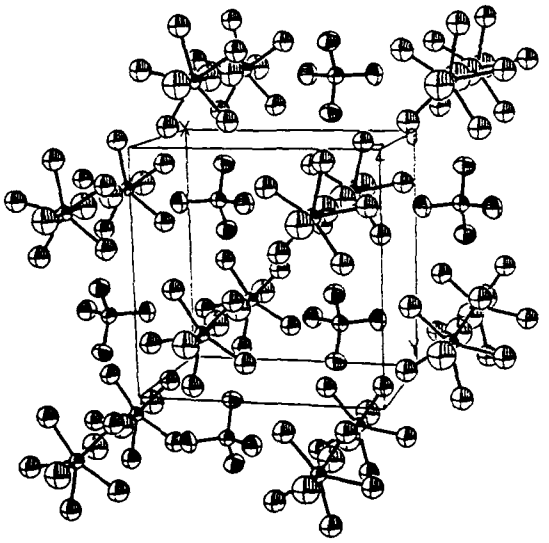

Figure 1. Packing diagram of $N(CH_3)_4^+IOF_6^-$ viewed along the c axis.

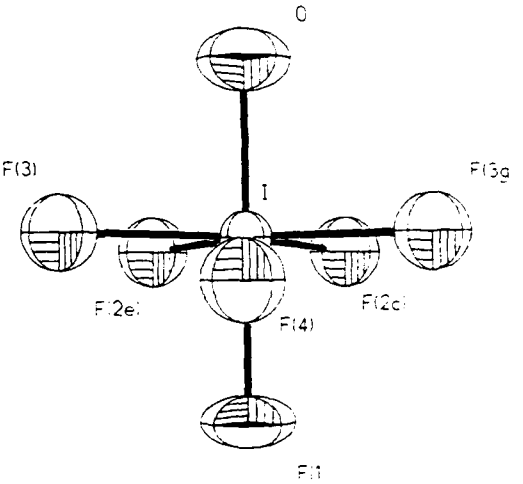

Figure 2. The structure of the IOF_6^- anion showing the puckering pattern of the equatorial fluorine ligands.

$$N(CH_3)_4^+F^- + IOF_5 \xrightarrow{CH_3CN} N(CH_3)_4^+IOF_6^- \qquad (1)$$

The resulting $N(CH_3)_4^+IOF_6^-$ is a very pale yellow solid which is thermally stable up to about 137 °C where it starts to decompose to IOF_4^-, CF_4, and COF_2 as the major products. It was characterized by elemental analysis, a crystal structure determination, and vibrational and ^{19}F NMR spectroscopy (see below).

X-ray Crystal Structure of $N(CH_3)_4^+IOF_6^-$. The crystal structure of $N(CH_3)_4^+IOF_6^-$ at −93 °C was determined at McMaster University and confirmed at the Freie Universität Berlin for a crystal kept at −155 °C. Although the gross features of both structures are very similar, they exhibit an extremely interesting temperature dependence of the degree of puckering and, therefore, both data sets are given in full detail.

The crystal structure of $N(CH_3)_4^+IOF_6^-$ consists of well-separated $N(CH_3)_4^+$ and IOF_6^- ions. The packing of the ions (see Figure 1) can be described as a cubic close packing of alternating layers of IOF_6^- anions and $N(CH_3)_4^+$ cations in which the alternating orientation of the tetrahedral cations results in a cuboctahedral[37] unit cell with $Z = 2$. While the cation is perfectly ordered with the expected bond lengths, the IOF_6^- anion is subject to a positional 4-fold disorder in the equatorial plane. The model results from the superposition of four anions in which the central I atom and the axial O and F(1) atoms occupy identical positions.

(34) Sheldrick, G. M. *Program for Crystal Structure Determination*; Göttingen, 1976.
(35) *International Tables for X-ray Crystallography*; The Kynoch Press: Birmingham, 1968; Vol. III.
(36) Christe, K. O.; Wilson, W. W.; Wilson, R. D. *Inorg. Chem.* **1989**, *28*, 904.
(37) Hyde, B. G.; Anderson, S. *Inorganic Crystal Structures*; John Wiley & Sons: New York, 1989; p 7.

One of these anions is shown in Figure 2. There are no significant contacts to iodine other than the directly bonded oxygen and six fluorine ligands, and the anion exhibits a gross pentagonal bipyramidal geometry. The O–I–F_{ax} angle is constrained by symmetry to be 180°, while there are no constraints on the positions of the equatorial fluorines. The equatorial fluorines are bent away from the axial oxygen ligand, as expected for a doubly bonded oxygen being more repulsive than a singly bonded fluorine ligand.[5]

The I–O bond length (1.75–1.77 Å) indicates significant double bond character for the I–O bond.[38-43] Its temperature dependence will be discussed below. The greater I–O bond length in IOF_6^-, when compared with that in IOF_5 (1.715(4) Å),[38] is consistent with the placement of some of the negative charge on oxygen, thereby increasing the polarity and decreasing the bond order of the I–O bond. The axial I–F bond (1.823(3) Å) is, within experimental error ($\pm 3\sigma$), significantly shorter than all of the equatorial I–F bonds (average 1.88 Å), and both types of I–F bonds in IOF_6^- are significantly longer than the corresponding bonds in IF_7 (1.786(7) and 1.858(4) Å, respectively).[7] These differences can be attributed again to the formal negative charge on IOF_6^-, which leads to greater $I^{\delta+}$–$F^{\delta-}$ bond polarities and consequently longer bonds. The greater length of the equatorial bonds in IOF_6^- and IF_7 relative to their axial ones is due to the increased mutual repulsion of the fluorine ligands in the highly congested equatorial plane and their higher ionicity (see below).

Nature and Temperature Dependence of the Equatorial Puckering in IOF_6^-. As mentioned above, the equatorial fluorine atoms in IOF_6^- are bent away from the doubly bonded oxygen atom by about 5°. Furthermore, the plane of the equatorial fluorine atoms is puckered and its I–F bonds are elongated in order to lessen the high degree of ligand–ligand repulsion encountered for these fluorines. Contrary to the rapid dynamic puckering in free, pentagonal-bipyramidal molecules, such as IF_7,[8] the puckering in solid $N(CH_3)_4^+IOF_6^-$ is frozen out by hydrogen···fluorine bridging between the two F(2) atoms of IOF_6^- and hydrogen atoms from two different cations. This bridging results in two close F···C contacts of 3.175(9) and 3.271(9) Å, while the remaining closest F···C contacts occur at 3.317(9), 3.473(9), and 3.416(9) Å and are very close to the accepted sum of the van der Waals radii of CH_3 (2.00 Å)[44] and F (1.35–1.40 Å)[44,45] which is 3.35–3.40 Å.

A pentagonal plane can be puckered in two ways resulting in structures of either C_s or C_2 symmetry, respectively.

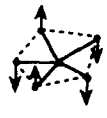

C_s

C_2

As mentioned above, the doubly bonded, axial oxygen ligand in IOF_6^- is more repulsive than the singly bonded, axial fluorine ligand. Therefore, the average equatorial plane, which can be defined as a plane perpendicular to the O–I–F_{ax} axis containing all five equatorial fluorine ligands at the averaged F_{eq}–I–O bond angle, drops below the center of the iodine atom. As can be seen from Table II and Figure 2, the puckered plane of IOF_6^- definitely exhibits C_s symmetry.

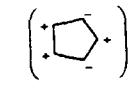

Furthermore, the relative displacements of the equatorial fluorine ligands from the average equatorial plane decrease with decreasing temperature, i.e. *the degree of puckering decreases with decreasing temperature*.

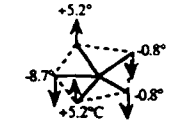

-93 °C

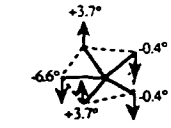

-155 °C

This decrease in the degree of puckering at lower temperatures causes additional important structural changes. Thus, the I–O bond length is significantly shortened and the angle between the oxygen ligand and the average equatorial plane is increased.

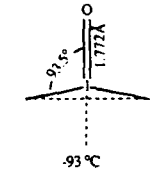

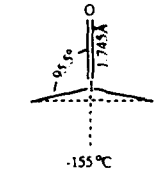

These temperature effects can be explained by a decreasing population of the higher vibrational states of the ring puckering motion which, due to its low frequency of about 141 cm^{-1}, is, even at low-temperatures, still highly populated. The resulting decrease in the thermal motion of the equatorial fluorines diminishes their mutual repulsion and allows the equatorial fluorines to become more coplanar and less repulsive which, in turn, results in a shortening of the I–O bond length. It would therefore be of great interest to determine the crystal structure of $N(CH_3)_4^+IOF_6^-$ at a very low temperature at which the puckering motion is completely frozen out and to compare the resulting structure with those of the present study. Such a study could establish beyond a doubt that in their minimum energy structures these normally puckered, pentagonal bipyramidal molecules indeed possess unpuckered equatorial planes.

^{19}F NMR Spectrum of the IOF_6^- Anion. The ^{19}F NMR spectrum (obtained at McMaster University) of $N(CH_3)_4^+IOF_6^-$ was recorded at –40 °C in CH_3CN solution and is in agreement with a pentagonal bipyramidal structure for the IOF_6^- anion. This structure is expected to have an average C_{5v} point group symmetry with the oxygen in the axial position. Accordingly, the ^{19}F NMR spectrum (Figure 3) displays a broad doublet ($\Delta\nu_{1/2} \approx 170$ Hz) at 166.0 ppm, assigned to the equatorial fluorines, and a broad binomial sextet ($\Delta\nu_{1/2} \approx 360$ Hz) at 111.1 ppm, assigned to the axial fluorine *trans* to oxygen. The weak triplet observed at 114.5 ppm [$^2J(F_{eq}$–$F_{ax}) = 200$ Hz] is attributed to the F-*trans*-to-O environment of *cis*-$IO_2F_4^-$ [46] which probably arose from adventitious hydrolysis of IOF_6^- during synthesis or NMR sample preparation. The observation of separate ^{19}F resonances for the axial and equatorial ligand environments of IOF_6^- is unusual for a pentagonal bipyramidal species and demonstrates that the IOF_6^- anion does not undergo intramolecular ligand exchange (i.e., pseudorotation) in solution, in contrast with the related TeF_7^- anion[10,11] and IF_7 molecule.[47] This is not surprising because any plausible intermediate in the pseudorotation process for IOF_6^- would require the doubly bonded oxygen ligand to move into an

(38) Bartell, L. S.; Clippard, F. B.; Jacob, J. E. *Inorg. Chem.* **1976**, *15*, 3009.
(39) Smart, L. E. *J. Chem. Soc., Chem. Commun.* **1977**, 519.
(40) Selte, K.; Kjekshus, A. *Acta Chem. Scand.* **1970**, *24*, 1912.
(41) Kálmán, K.; Cruickshank, D. W. J. *Acta Crystallogr.* **1970**, *B26*, 1782.
(42) Feikeman, Y. D. *Acta Crystallogr.* **1961**, *14*, 315.
(43) Feikeman, Y. D. *Acta Crystallogr.* **1966**, *20*, 765.
(44) Pauling, L. *The Nature of the Chemical Bond*, 3rd ed.; Cornell University Press: Ithaca, New York, 1960; p 260.
(45) Bondi, A. *J. Phys. Chem.* **1964**, *68*, 441.
(46) Christe, K. O.; Wilson, R. D.; Schack, C. J. *Inorg. Chem.* **1981**, *20*, 2104.
(47) (a) Gillespie, R. J.; Quail, J. W. *Can. J. Chem.* **1964**, *42*, 2671. (b) Bartlett, N.; Beaton, S.; Reeves, L. W.; Wells, E. J. *Can. J. Chem.* **1964**, *42*, 2531. (c) Alexakos, L. G.; Cornwell, C. D.; Pierce, St. B. *Proc. Chem. Soc.* **1964**, *86*, 293. (d) Gutowski, H. S.; Hoffmann, C. F. *J. Chem. Phys.* **1951**, *19*, 1259.

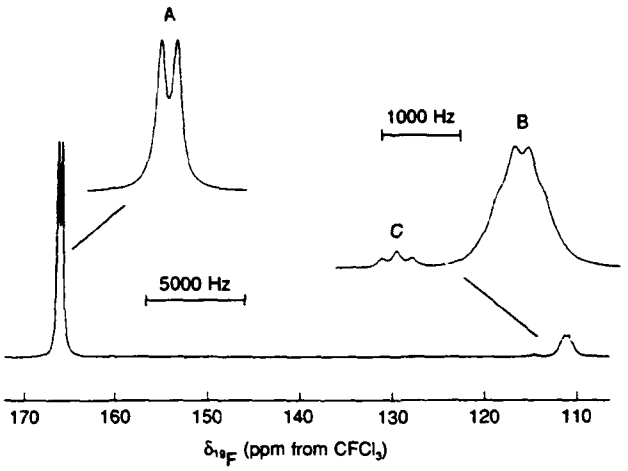

Figure 3. The ^{19}F NMR spectrum (470.599 MHz) of a saturated solution of $N(CH_3)_4^+IOF_6^-$ in CH_3CN at −40 °C: (A) F_{eq} environment of IOF_6^-; (B) F_{ax} environment of IOF_6^-; (C) F-*trans*-to-O environment of *cis*-$IO_2F_4^-$ impurity.

equatorial position. The greater space requirement of the oxygen double bond domain, compared with that of a fluorine single bond domain, would render the placement of the oxygen ligand in the more sterically crowded equatorial position energetically unfavorable, thereby creating a high activation barrier for the process. Although the X-ray crystal structure reveals that, in the solid state, the equatorial fluorine ligands of the IOF_6^- anion are unevenly puckered, only a single resonance is observed for these ligands in the ^{19}F NMR spectrum of the solution. Clearly, the puckering, which is frozen out in the solid state, becomes a dynamic process in solution which is fast on the NMR time scale.

It is of interest to compare the ^{19}F chemical shifts of IOF_6^- with those of other related iodine(VII) oxofluoro species. The ^{19}F chemical shifts of the F-*trans*-to-F environments in *trans*-$IO_2F_4^-$, *cis*-$IO_2F_4^-$,[46] and IOF_5[47] occur in a specific region at 65.1, 66.0, and 68 ppm, respectively. Similary, the ^{19}F chemical shifts of the F-*trans*-to-O environments in *cis*-$IO_2F_4^-$ and IOF_5 also occur in a distinct region at 112.8[46] and 107 ppm,[48] respectively. In the IOF_6^- anion it can be seen that the F-*trans*-to-O environment (111.1 ppm) also resonates in this region but that the resonance of the five equatorial fluorines (166.0 ppm) is strongly deshielded (i.e., by ca. 100 ppm) from the F-*trans*-to-F environments of IOF_5 and *cis*-/*trans*-$IO_2F_4^-$. This phenomenon has also been noted for the XeF_5^- anion in which the fluorines in the pentagonal plane resonate 56.8 ppm to high frequency of the fluorine ligands in square-planar XeF_4.[49] In the cases of the pentagonal bipyramidal TeF_7^- anion and IF_7 molecule, even at low temperature[10,11,47] only average ^{19}F chemical shifts can be obtained owing to their fluxional behavior. Nevertheless, the fact that these average chemical shifts occur at significantly higher frequency than those of the related octahedral TeF_6[50] and IF_6^+[51] species indicates that the five equatorial fluorines have a higher frequency ^{19}F chemical shift than the two axial fluorine ligands, since the former will contribute the largest weighting to the average chemical shift.

The large chemical shift differences between fluorine ligands in a square plane and those in a pentagonal plane in the aforementioned species are indicative of the dominance of the paramagnetic contribution to the ^{19}F shielding constant. In the theory developed by Pople and Karplus,[52] the paramagnetic contribution to the shielding constant of an atom A bonded to another atom B is given by eq 2

$$\sigma_p^A = \frac{-e^2\hbar^2\langle r^{-3}\rangle_{2p}}{2m^2c^2\Delta E}[Q_{AA} + \sum_{B\neq A} Q_{AB}] \qquad (2)$$

where $\langle r^{-3}\rangle_{2p}$ is the mean inverse cube of the 2p-orbital radial function on atom A, Q_{AA} is the charge density term for atom A, Q_{AB} is the bond order term for the A–B bond, and ΔE is the mean excitation energy.

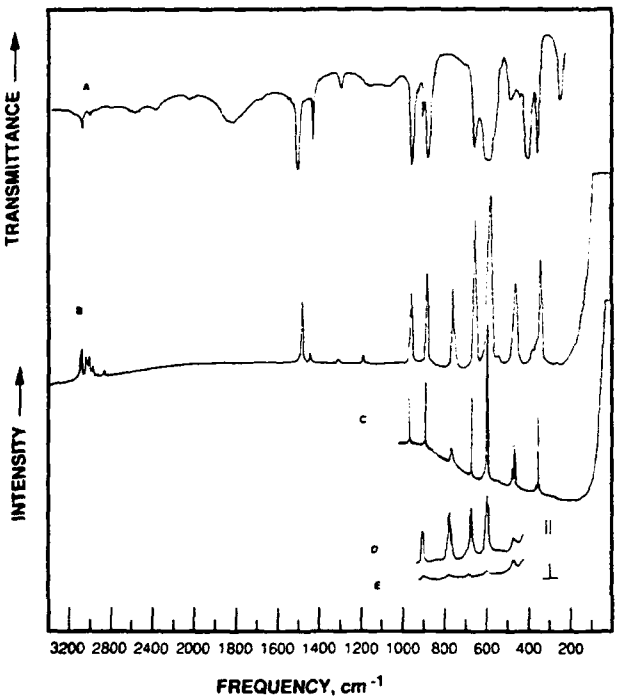

Figure 4. Vibrational spectra of $N(CH_3)_4^+IOF_6^-$. Trace A, infrared spectrum of the solid as an AgBr disk; traces B and C, Raman spectra of the solid at 25 and −146 °C; traces D and E, Raman spectra of the CH_3CN solution with parallel and perpendicular polarization, respectively.

Compared with the bonds in the corresponding octahedral or pseudooctahedral precursors, $MO_xF_x^n$, those in the $MO_xF_{x+1}^{n-1}$ species, which contain a pentagonal plane of M–F bonds (where M = Xe, I, Te), exhibit greater ionic character, as indicated by their longer bond lengths and lower vibrational stretching frequencies. This greater ionic character would be expected to bring about a decrease in the $\langle r^{-3}\rangle_{2p}$ and charge density–bond order terms of eq 2. This would result in a decrease in σ_p and a more shielded chemical shift and does not account for the experimentally observed trend. Consequently, it would appear that the origin of the observed deshielding most likely lies in the ΔE term. Unfortunately, the nature of the excited states is unknown at present; however, it is interesting to note that comparison of the HOMO energies in XeF_4 and XeF_5^- [49] as well as IOF_5 and IOF_6^- reveals that the anions have significantly lower values than the neutral molecules and may facilitate excitation to a higher excited state, i.e., ΔE is smaller for XeF_5^- and IOF_6^- than for XeF_4 and IOF_5.

The two-bond fluorine–fluorine scalar coupling $^2J(^{19}F_{ax}-^{19}F_{eq})$ in IOF_6^- has a value of 205 Hz and is almost identical in magnitude to that measured previously for *cis*-$IO_2F_4^-$ in CH_3CN [$^2J(^{19}F_{ax}-^{19}F_{eq})$ = 204 Hz].[46] The couplings in both anions are smaller than the corresponding coupling in the related IOF_5 molecule [$^2J(^{19}F_{ax}-^{19}F_{eq})$ = 271–280 Hz],[53] which may reflect the anticipated greater ionic character in the bonds of the anionic species.[54] In the ^{19}F NMR spectrum of IOF_6^-, both the doublet and sextet

(48) Remeasured for this work in CH_3CN at −40 °C.
(49) Christe, K. O.; Curtis, E. C.; Dixon, D. A.; Mercier, H. P.; Sanders, J. C. P.; Schrobilgen, G. J. *J. Am. Chem. Soc.* **1991**, *113*, 3351.
(50) This work; chemical shift determined as δ = −51.3 ppm for TeF_6 in CH_3CN at −40 °C.
(51) Brownstein, M.; Selig, H. *Inorg. Chem.* **1972**, *11*, 656.
(52) Karplus, M.; Pople, J. A. *J. Chem. Phys.* **1963**, *38*, 2803.
(53) Brownstein, M.; Gillespie, R. J.; Krasznai, J. P. *Can. J. Chem.* **1978**, *56*, 2253.

Table III. Vibrational Spectra of $N(CH_3)_4^+IOF_6^-$ and Their Assignment

obsd freq, cm^{-1} (rel intensity)				assignments (point group)	
	Ra				
	solid		CH_3CN sol		
IR 25 °C	25 °C	−150 °C	25 °C	$N(CH_3)_4^+$ (T_d)	IOF_6^- (C_{5v})
3045 mw	3043 (20)	3045 (5)		$\nu_5(E)$	
	2996 (13)				
2970 w	2965 (13)	2970 (4)		$\nu_{14}(F_2)$	
	2927 (6)			$\nu_1(A_1)$ + combin bands	
	2819 (5)				
1489 vs				$\nu_{15}(F_2)$	
	1464 (46)	1466 (15)		$\nu_2(A_1)$, $\nu_6(E)$	
1418 m	1417 (6)	1416 (3)		$\nu_{16}(F_2)$	
1285 mw	1288 (3)			$\nu_{17}(F_2)$	
	1173 (6)	1174 (4)		$\nu_7(E)$	
949 vs	948 (41)	949 (28)		$\nu_{18}(F_2)$	
873 vs	874 (53)	873 (37)	880 (50) p		$\nu_1(A_1)$
	752 (45)	753 (15)		$\nu_3(A_1)$	
	740 sh	742 sh			
649 s	649 (88)	658 (57)	656 (75) p		$\nu_2(A_1)$
585 vs					$\nu_5(E_1)$
	578 (100)	584 (100)	581 (100) p		$\nu_3(A_1)$
535 w,sh	530 (4)	530 (3)			$\nu_9(E_2)$
490 m		466 (15)		$\nu_{19}(F_2)$	
475 sh					
	457 (49)	456 (23)	457 (20) dp		$\nu_{10}(E_2)$
405 vs					$\nu_6(E_1)$
	373 sh	377 (5)		$\nu_8(E)$	
359 s		354 (4)			$\nu_4(A_1)$
	341 (62)	344 (52)			$\nu_7(E_1)$
		335 (5)		$\nu_{12}(F_1)$	
255 s	260 (2)	260 (2)			$\nu_8(E_1)$

are significantly broadened owing to partially collapsed scalar coupling to the quadrupolar ^{127}I ($I = 5/2$) nucleus. The ^{19}F NMR spectra of *cis*-$IO_2F_4^-$ [46] and IOF_5[47a] also show broadening attributed to the same cause. Interestingly, the line width of the sextet of IOF_6^- is substantially broader than that of the doublet, indicating that $^1J(^{19}F_{ax}-^{127}I)$ is larger than $^1J(^{19}F_{eq}-^{127}I)$ and therefore less quadrupole collapsed. If it is assumed that the Fermi-contact mechanism provides the dominant coupling contribution, then this observation is consistent with the relatively more covalent (i.e., greater s-character) bond between iodine and the axial fluorine as compared with those between iodine and the equatorial fluorines.[54] The X-ray crystallographic data and vibrational spectra for $N(CH_3)_4^+IOF_6^-$ support this idea in that the $I-F_{ax}$ bond distance is shorter than the average $I-F_{eq}$ bond distance and the $I-F_{ax}$ force constant is larger than the $I-F_{eq}$ one (see below).

Vibrational Spectra. The infrared and Raman spectra of solid $N(CH_3)_4^+IOF_6^-$ and the Raman spectra of its CH_3CN solution were recorded and are shown in Figure 4. The observed frequencies, together with their assignments, are summarized in Table III. A comparison of the observed and calculated (see below) frequencies of IOF_6^- with those of the closely related pentagonal IF_7 molecule[8] and XeF_5^- anion,[49] together with their approximate mode descriptions, is given in Table IV. After subtraction of the well-known[15,55] bands of the $N(CH_3)_4^+$ cation (see Table III), the remaining bands, which are due to IOF_6^-, can be readily assigned based on the data given in Table IV. Since the vibrational spectra of IOF_6^- in solid $N(CH_3)_4^+IOF_6^-$ do not appear to be noticeably affected by the slight equatorial puckering, they were assigned (see Table IV) in point group C_{5v} which is the lowest energy structure of the free anion (see below).

Ab Initio Calculations and Normal Coordinate Analyses. The electronic structure of IOF_6^- was calculated at the ab initio level by using both local density functional (LDF) theory and molecular orbital theory with an effective core potential (ECP) for the core electrons of iodine. Both types of calculations resulted in minimum energy structures of C_{5v} symmetry with the ECP calculations duplicating the experimentally observed geometry (see Table V) and vibrational frequencies (see Table IV) much better than the LDF calculations. In view of the superiority of the ECP calculations, we have also recalculated the structure of the closely related XeF_5^- anion, for which previously[49] only LDF values had been available. As can be seen from Tables IV and V, the ECP calculations are in excellent agreement with the observed values, after scaling of the calculated frequencies by empirical factors to maximize their fit with the experimental data, and therefore are invaluable for the correct assignments of the vibrational spectra. For XeF_5^-, for example, they clearly indicate that the previous assignments[49] for $\nu_2(A_2'') = 274\ cm^{-1}$ and $\nu_4(E_1') = 290\ cm^{-1}$ should be reversed. In view of the closeness of these two frequencies, the reversal of their assignments has very little or no impact on the conclusions previously reached[49] for XeF_5^-.

The eleven fundamental vibrations of a pentagonal bipyramidal AX_5YZ species in point group C_{5v} can be classified as $\Gamma = 4A_1$(IR,Ra) + $4E_1$(IR,Ra) + $3E_2$(Ra). The internal coordinates, symmetry coordinates, and approximate mode descriptions for IOF_6^- are summarized in Figure 5 and Table S6, respectively. The tentative assignments given in our preliminary communication[10] for IOF_6^- and IF_7 have been significantly improved resulting in revised assignments for ν_6, ν_7, ν_8, and ν_{10} of IOF_6^- and for ν_9 and ν_{10} of IF_7.

By the use of the scaled ECP frequencies, force fields were calculated for IOF_6^- (see Table VI) and XeF_5^- (see Table VII). The potential energy distribution (PED) for IOF_6^- is given in Table VIII. As can be seen from Table VIII, the IF_5 in-plane deformation motions, due to their high frequencies, mix considerably with some of the other symmetry coordinates, and the $\nu_7(E_1)$ and $\nu_8(E_1)$ modes are antisymmetric and symmetric combinations, respectively, of S_7 and S_8. Consequently, ν_7 and ν_8 are better described as an $O-I-F_{ax}$ rocking motion

(54) Jameson, C. J. In *Multinuclear NMR*; Mason, J., Ed.; Plenum Press: New York, 1987; Chapter 4, pp 97–101.
(55) Christe, K. O.; Wilson, W. W.; Bau, R.; Bunte, S. W. *J. Am. Chem. Soc.* **1992**, *114*, 3411 and references cited therein.

and an O–I–F_{ax} scissoring motion

respectively, than as separated I=O and I—F_{ax} wagging motions. The only deficiency of the ECP calculation for IOF_6^- was the low-frequency value and resulting force constant for the scaled I–O stretching mode, $\nu_1(A_1)$. Consequently, we prefer to use for this mode the unscaled value of 860 cm^{-1} which is in much better agreement with the observed value of 873 cm^{-1}. The low value calculated for this stretching frequency is surprising as the calculated I–O bond length is shorter than the experimental value. Due to the larger number of symmetry species for XeF_5^-, its PED (see Table VII) is highly characteristic and requires no further comment. It should be noted, however, that the symmetry coordinates and internal force constants, previously published[49] for XeF_5^-, contained two typographical errors. S_{5b} should read $(2/5)^{1/2}$ [sin 2α ($\Delta r_2 - \Delta r_5$) – sin α ($\Delta r_3 - \Delta r_4$)], and subscripts had been omitted from the last two internal force constants in Table VIII which should read $f_{\gamma\gamma} - f_{\gamma\gamma}'$ and $f_{\gamma} - f_{\gamma\gamma}$, respectively.

The internal force constants of greatest interest are those involving the stretching of the axial and the equatorial fluorine bonds and the equatorial in-plane deformation constants. These data are summarized for the IF_7, IOF_6^-, XeF_5^- series in Table IX. As can be seen from this table, the X–F_{ax} bonds are considerably stronger than the X–F_{eq} ones for a given compound, as expected from the bonding scheme proposed below. Furthermore, the stretching force constants decrease significantly on going from IF_7 to IOF_6^- and XeF_5^-, as expected from an increasing ionicity of the X–F bonds caused by the formal negative charge in the anions and the reduction in the formal oxidation state of the central atom from +VII in IF_7 and IOF_6^- to +IV in XeF_5^-. The large increase in the value of f_{rr}', the coupling to opposite bonds, from IOF_6^- to XeF_5^-, is analogous to those previously observed[46] for going from either *trans*-$IO_2F_4^-$ (f_{rr}' = 0.27 mdyn/Å) to IOF_4^- (f_{rr}' = 0.45 mdyn/Å) and IF_4^- (f_{rr}' = 0.47 mdyn/Å) or IOF_5^- (f_{rr}' = 0.18 mdyn/Å) to IF_5 (f_{rr}' = 0.38 mdyn/Å) and, hence, appears to be associated with the introduction of a sterically active, free valence electron pair into the ligand sphere around the central atom.

The in-plane deformation constants, f_α, are a measure for the strength of the mutual repulsion of the equatorial ligands and hence for the degree of congestion in this plane which, in turn, is responsible for the puckering. As can be seen from Table IX, the value of f_α decreases markedly on going from IF_7 to IOF_6^- and XeF_5^-. In IF_7, the in-plane deformation constant, f_α, is about five times larger than the out-of-plane deformation constant, f_β, and accounts for the puckering of the equatorial plane in IF_7. On the other hand, in XeF_5^- the f_α value has become much smaller and approaches the range of values expected for the out-of-plane deformation constants, f_β. This is in good agreement with the X-ray crystal structure of $N(CH_3)_4^+XeF_5^-$ which showed[49] that XeF_5^- is planar and not puckered. Hence, it appears that the value of the in-plane deformation force constant, f_α, is a useful parameter for measuring the degree of congestion and the likely occurrence of puckering in the equatorial ligand plane.

It must be pointed out that the problem of calculating the internal deformation constants from the corresponding symmetry force constants is underdetermined (more unknowns than available equations) and, hence, requires additional assumptions. For the calculation of f_α in our compounds, the pure vibrational force field[56] condition of Kuczera, adapted to 5-fold symmetry, f_α +

(56) (a) Kuczera, K.; Czerminski, R. *J. Mol. Struct.* **1983**, *105*, 269. (b) Kuczera, K. *J. Mol. Struct.* **1987**, *160*, 159.

Table IV. Comparison of Observed and Calculated Frequencies of IOF_6^-, IF_7, and XeF_5^-, Together with Their Approximate Mode Descriptions

	IOF_6^- (C_{5v})				IF_7 (D_{5h})[a]					XeF_5^- (D_{5h})				
		obsd	calcd freq, cm^{-1}			obsd	calcd freq, cm^{-1}				obsd	calcd freq, cm^{-1}	
assign	approx mode description	freq, cm^{-1} int (IR,Ra)	ECP[c]	LDF	assign	approx mode description	freq, cm^{-1} int (IR,Ra)	ECP[c]	LDF	assign	approx mode description	freq, cm^{-1} int (IR,Ra)	ECP[d]	LDF[f]
A_1 ν_1	ν I=O	873 (vs,53p)	860[b]	870	$\nu_3(A_2'')$	ν as IF_2ax	746 (s,–)	753	710					
ν_2	ν IF_{ax}	649 (s,88p)	625	599	$\nu_1(A_1')$	ν sym IF_2ax	676 (–,20p)	673	630					
ν_3	ν sym IF_5	584 (ν_5,100p)	566	537	$\nu_2(A_1')$	ν sym IF_5	635 (–,100p)	644	598	$\nu_1(A_1')$	ν sym XeF_5	502 (–,100)	498	467
ν_4	δ umbrella IF_5	359 (s,4)	371	314	$\nu_4(A_2'')$	δ umbrella IF_5	365 (s,–)	368	304	$\nu_2(A_2'')$	δ umbrella XeF_5	290 (m,sh,–)	301	270
E_1 ν_5	ν as IF_5	585 (ν_8,ν_3)	583	568	$\nu_5(E_1')$	ν as IF_5	670 (vs,–)	681	647	$\nu_3(E_1')$	ν as XeF_5	450 (vs,–)	449	502
ν_6	δ as IF_5 in plane	405 (vs,–)	415	365	$\nu_6(E_1')$	δ as IF_5 in plane	425 (vs,–)	441	377	$\nu_4(E_1')$	δ as XeF_5 in plane	274 (s,–)	273	248
ν_7	δ rock O=I—F_{ax}	341 (–,62)	340	292	$\nu_8(E_1'')$	δ rock IF_2ax	319 (–,6)	320	259					
ν_8	δ sciss O=I—F_{ax}	260 (s,2)	273	233	$\nu_7(E_1')$	δ sciss IF_2ax	257 (w,–)	265	213					
E_2 ν_9	δ sciss IF_5 in plane	530 (–,4)	530	486	$\nu_9(E_2')$	mixture of δ sciss	596 (–,2)	605	561	$\nu_5(E_2')$	ν as XeF_5	423 (–,16)	420	413
ν_{10}	ν as IF_5	457 (–,49)	446	421	$\nu_{10}(E_2'')$	in plane and ν as IF_5	510 (–,17)	515	467	$\nu_6(E_2')$	δ sciss XeF_5 in plane	377 (–,23)	373	375
ν_{11}	δ pucker IF_5	not obsd	141	111	$\nu_{11}(E_2'')$	δ pucker IF_5	[68]	59	50i	$\nu_7(E_2'')$	δ pucker XeF_5	not obsd	105	79

[a] Frequency values were scaled by an empirical factor of 0.9038. [b] Unscaled frequency value; scaled frequency value is 789 cm^{-1}. [c] Frequency values were scaled by an empirical factor of 0.932. [d] Frequency values were scaled by an empirical factor of 0.8618. [e] Data from ref 8. [f] Data from ref 49.

Table V. Observed and Calculated Geometries of IOF_6^- and the Closely Related IF_7 and XeF_5^-

IOF_6^-				IF_7				XeF_5^-			
		calcd[a]				calcd[c]				calcd	
	exp[a]	ECP	LDF		exp[b]	ECP	LDF		exp[d]	ECP	LDF
rI–O (Å)	1.75–1.77	1.7255	1.791	rI–F_{ax}	1.781	1.7705	1.870	rXe–F_{eq}	2.012	1.9924	2.077
rI–F_{ax} (Å)	1.82	1.8087	1.913	rI–F_{eq}	1.857	1.8333	1.918				
rI–F_{eq} (Å)	1.88	1.8819	1.969	F_{ax}–I–F_{eq}	90	90	90				
O–I–F_{eq} (deg)	94–96	95.76	96.0								

[a] Data from this study. [b] Data from ref 7. [c] Data from ref 8. [d] Data from ref 49.

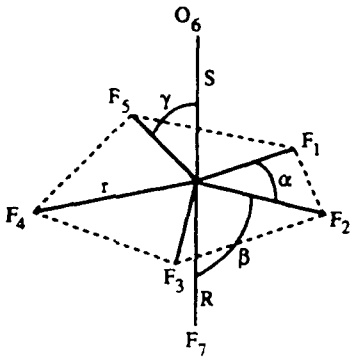

Figure 5. Internal coordinates for IOF_6^-.

Table VI. Symmetry Force Constants[a] of IOF_6^- Calculated from the Scaled ECP Frequencies of Table IV

		F_{11}	F_{22}	F_{33}	F_{44}
A_1	F_{11}	6.077[b] (4.967)[c]			
	F_{22}	0.057	3.899		
	F_{33}	–0.041	0.169	3.656	
	F_{44}	–0.164	0.332	0.078	1.725
		F_{55}	F_{66}	F_{77}	F_{88}
E_1	F_{55}	3.040			
	F_{66}	–1.079	3.246		
	F_{77}	0.230	–0.234	1.087	
	F_{88}	0.176	–0.271	0.085	0.891
		F_{99}	$F_{10,10}$	$F_{11,11}$	
E_2	F_{99}	2.844			
	$F_{10,10}$	0.407	2.478		
	$F_{11,11}$	–0.007	–0.064	0.395	

[a] Stretching constants in mdyn/Å, deformation constants in mdyn Å/rad^2, and stretch–bend interaction constants in mdyn/rad. [b] Unscaled value (see text). [c] Scaled value.

$2f_{\alpha\alpha} + 2f_{\alpha\alpha'} \equiv 0$, was used. Since for f_β the case is even more complex, no explicit values were calculated for f_β of IOF_6^- and XeF_5^-; however, we estimate f_β of IOF_6^- to be slightly larger than and that of XeF_5^- to be similar to that of IF_7.

Structure and Bonding in IOF_6^- and Related Molecules and Ions. The pentagonal bipyramidal structure and the co-planarity of the equatorial ligands in the minimum energy configuration of IOF_6^-, which cannot be accounted for by either "repelling points on a sphere" VSEPR arguments[5] or classical, directionally localized molecular orbitals, can be rationalized in terms of a bonding scheme, outlined[49] for XeF_5^- and elaborated on in more detail[8] for IF_7. In this scheme, the structure and bonding of XeF_5^- are explained by a simple model derived from XeF_4. The bonding in the square-planar XeF_4 can be described by two semi-ionic, 3-center 4-electron (3c–4e) bonds[57] for the four Xe–F bonds and two lone valence electron pairs on Xe ($s^2p_z^2$ hybrids). The 3c–4e bonds involve the p_x^2 and p_y^2 orbitals of xenon. Addition of an F^- ion to the equatorial plane in XeF_4 results in pentagonal-planar XeF_5^- and the formation of a semi-ionic, 6-center 10-electron (6c-10e) bond involving the delocalized $p_x^2p_y^2$ hybrid orbitals of Xe and 6 electrons on the 5 F ligands.[49] The two lone valence electron pairs on Xe in XeF_5^- are analogous to those in XeF_4.

Now let us consider the bonding in IF_7 and IOF_6^-. Their planar IF_5 fragments have essentially the same bonding as XeF_5^-, as shown by the atomic population calculations given in Table X. As expected for the replacement of two free valence electron pairs on the central atom by two bonded ligands, each of which

(57) (a) Pimentel, G. C. *J. Chem. Phys.* **1951**, *10*, 446. Hach, R. J.; Rundle, R. E. *J. Am. Chem. Soc.* **1951**, *73*, 4321. Rundle, R. E. *J. Am. Chem. Soc.* **1963**, *85*, 112. (b) Burdett, J. K. In *Molecular Shapes: Theoretical Models of Inorganic Stereochemistry*; Wiley: New York, 1980.

Table VII. Revised Assignments, ECP Force Field,[a] and Potential Energy Distribution[b] for XeF_5^-

assign		approx mode description	freq cm^{-1} calcd (ECP)	freq cm^{-1} obsd[c]	symmetry force constants	PED
A_1	ν_1	ν sym XeF_5	498	502	F_{11} = 2.775	100(1)
A_2''	ν_2	δ umbrella	301	290	F_{22} = 1.191	100(2)
E_1'	ν_3	ν asym XeF_5	449	450	F_{33} = 1.6714	97(3) + 3(4)
					F_{34} = –0.193	
	ν_4	δ asym in plane	273	274	F_{44} = 1.940	99(4) + 1(3)
E_2'	ν_5	ν asym XeF_5	420	423	F_{55} = 1.938	92(5) + 8(6)
					F_{56} = 0.1191	
	ν_6	δ in-plane	373	377	F_{66} = 1.7505	91(6) + 9(5)
E_2''	ν_7	δ pucker	105		F_{77} = 0.2498	100(7)

[a] Force constants calculated with the ECP frequencies; stretching constants in mdyn/Å, deformation constants in mdyn Å/rad^2, and stretch–bend interaction constants in mdyn/rad. [b] PED in percent. [c] Data from ref 49.

Table VIII. Potential Energy Distribution for IOF_6^-

		freq, cm^{-1}	PED, %
A_1	ν_1	860	87(1) + 7(2) + 5(4)
	ν_2	625	83(2) + 10(3) + 4(1) + 2(4)
	ν_3	566	88(3) + 12(2)
	ν_4	371	100(4)
E_1	ν_5	583	97(5) + 2(8)
	ν_6	415	44(6) + 26(8) + 25(7) + 5(5)
	ν_7	340	58(8) + 42(7)
	ν_8	273	43(8) + 40(7) + 16(6)
E_2	ν_9	530	73(9) + 27(10)
	ν_{10}	446	72(10) + 28(9)
	ν_{11}	141	100(11)

Table IX. Internal Force Constants[a,b] (mdyn/Å) of IF_7, IOF_6^-, and XeF_5^-

	IF_7	IOF_6^-	XeF_5^-
f_R	5.005	3.897	
f_r	3.947	2.938	2.062
f_{rr}	0.326	0.306	0.198
$f_{rr'}$	0.0265	0.0536	0.317
f_α	0.847	0.690	0.364
$f_{\alpha\alpha}$	–0.183	–0.147	–0.081
$f_{\alpha\alpha'}$	–0.240	–0.198	–0.102
f_β	0.163		

[a] The deformation constants have been normalized for the following bond distances: IF_7, rI–F_{eq} = 1.857 Å; IOF_6^-, rI–F_{eq} = 1.877 Å; XeF_5^-, rXe–F = 2.0124 Å. [b] f_{rr} and $f_{rr'}$ denote coupling to adjacent and opposite bonds, respectively, and $f_{\alpha\alpha}$ and $f_{\alpha\alpha'}$ coupling to adjacent and opposite bond angles, respectively.

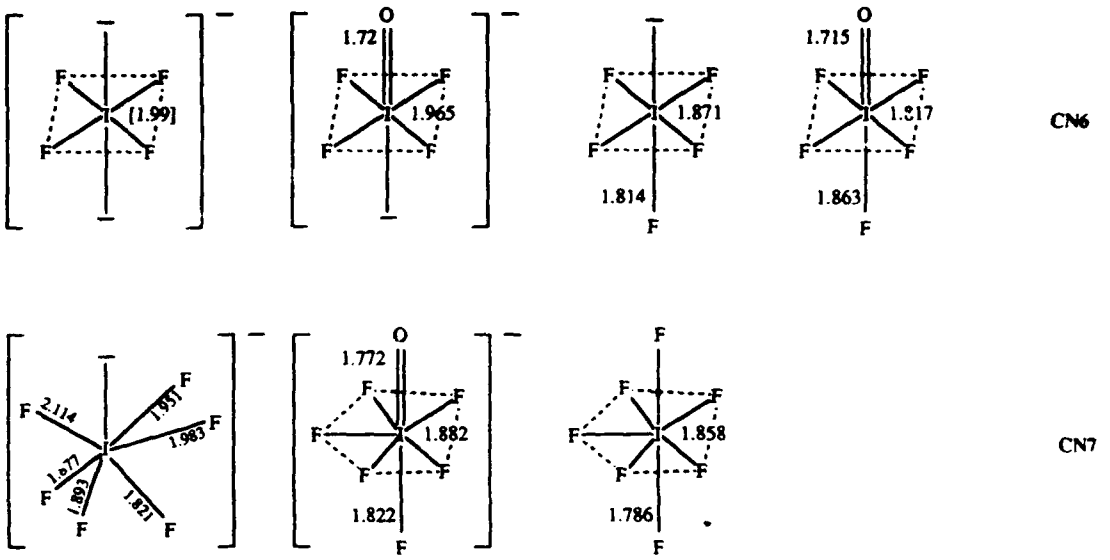

Figure 6. A comparison of the structure of IOF_6^- with those of closely related hexa- and heptacoordinated iodine fluorides and oxyfluorides.

Table X. Atomic Populations (e) in the Valence Electron Orbitals and Total Charge Distributions for XeF_5^-, IF_7, and IOF_6^-

	XeF_5^-	IF_7	IOF_6^-
	Central Atom		
s	2.22	1.35	1.43
$p_x = p_y$	0.61	0.64	0.64
p_z	2.02	0.60	0.71
d_{z^2}	0.03	0.11	0.14
$d_{x^2-y^2} = d_{xy}^2$	0.06	0.12	0.09
d_{xy}	0.14	0.20	0.16
$d_{xz} = d_{yz}$	0.04	0.14	0.15
d total	0.37	0.83	0.78
	Equatorial Fluorines		
s	1.98	1.93	1.94
p bond	1.70	1.57	1.64
p in plane	1.98	1.96	1.97
p_z	1.97	1.94	1.95
d	0	0.03	0.02
	Axial Fluorines and Oxygens		
s		1.92	1.92 (F), 1.86 (O)
p_z		1.54	1.57 (F), 1.16 (O)
$p_x = p_y$		1.94	1.95 (F), 1.83 (O)
d		0.04	0.03 (F), 0.04 (O)
	Total Charges		
central atom	2.15	2.94	2.81
F_{eq}	−0.63	−0.43	−0.53
F_{ax}		−0.39	−0.44
O_{ax}			−0.74

contributes one electron to its bond, the population of the s^2 and p_z^2 orbitals of I in IF_7 and IOF_6^- has decreased by about two electrons, compared to XeF_4 and XeF_5^-. The higher oxidation state of the central atoms in IF_7 and IOF_6^- (+VII) results in I having a higher positive charge than Xe (+IV) in XeF_5^-. This causes the effective electronegativity differences between the central atoms and the ligands in IF_7 and IOF_6^- to be smaller than those in XeF_4 and XeF_5^- and results in an increased covalency and a shortening of the central atom–fluorine bonds. Furthermore, the axial fluorine ligands in IF_7 and IOF_6^- carry less of a negative charge than the equatorial ones which accounts for the axial I–F bonds being more covalent and, hence, shorter than the equatorial ones. The total charge distributions in IF_7 and IOF_6^- (see Table X) also demonstrate the effect of replacing an F ligand in IF_7 by an O^- ligand. The oxygen substitution results in the release of electron density into the IF_6 part of the molecule which increases the negative charges on the six fluorines and weakens the I–F bonds in IOF_6^- relative to those in IF_7.

Of course, the above model does not account for the fact that the electrons will try to minimize their mutual repulsions and occupy all of the available orbitals to do so. This results in the participation of some d functions. Although we are not proposing a d hybridization model, the population in the d orbitals does suggest a redistribution into these orbitals beyond that expected if the d orbitals were to act solely as polarization functions.

The above atomic population and total charge distribution analysis qualitatively confirms our simple bonding model for pentagonal-bipyramidal molecules. This model involves the use of delocalized p_x^2 and p_y^2 hybrid orbitals of the central atom for the formation of a semi-ionic, 6c–10e bond with the five equatorial ligands and of an sp_z hybrid orbital for the formation of two, more covalent, axial bonds. This bonding scheme can account for all the observed structural features and also the observed bond length differences. The planarity of the p_x^2 and p_y^2 hybrid orbitals of the central atom also explains why these heptacoordinated main group fluorides and oxyfluorides prefer pentagonal-bipyramidal structures and not the monocapped octahedral or trigonal prismatic ones expected from VSEPR arguments.

As far as the puckering of the equatorial plane in pentagonal bipyramidal molecules is concerned, the data given above for IOF_6^- strongly suggest that the congestion in its equatorial plane and hence the driving force toward puckering is intermediate between those of puckered IF_7 and planar XeF_5^-. Therefore, it might be possible that by a reduction of the thermal motion of the ligands, the mutual repulsion among the equatorial ligands will be sufficiently diminished to allow for the observation of a temperature-dependent transition from a puckered to a planar configuration. Our two crystal structure determinations of $N(CH_3)_4^+IOF_6^-$ at different temperatures clearly demonstrate such a temperature dependency of the degree of puckering, and the ab initio calculations point to a minimum energy structure with coplanar equatorial ligands.

A comparison of the structure of IOF_6^- with those[7,38,58-61] of other hexa- and heptacoordinated iodine fluorides and oxyfluorides is shown in Figure 6 and suggests the following general effects: (i) If the central iodine atom possesses a free valence electron pair, this pair seeks high s character, i.e. sp^n hybridization. If the number of ligands is larger than four, then as many F ligands

(58) The bond length in IF_4^+ is a value estimated from a normal coordinate analysis: Christe, K. O.; Naumann, D. *Inorg. Chem.* **1973**, *12*, 59.
(59) Ryan, R. R.; Asprey, L. B. *Acta Crystallogr. Part B* **1972**, *B28*, 979.
(60) Balikci, B.; Brier, P. N. *J. Mol. Spectrosc.* **1981**, *89*, 254.
(61) Majhoub, A. R.; Seppelt, K. *Angew. Chem., Int. Ed. Engl.* **1991**, *30*, 323.

form semi-ionic, 3-center 4-electron (3c–4e)[57a] or similar multicenter bonds[57b] as are required to allow the free electron pairs to form an sp^n hybrid with any remaining ligands. The resulting semi-ionic, multi-center bonds are considerably longer than the more covalent sp^n hybrid bonds.[62] This effect accounts for the long equatorial I–F bonds in IF_4^-,[58] IOF_4^-,[59] and IF_5,[60] and the short axial I–F bond in IF_5.[60] (ii) If the central atom does not possess any free valence electron pair, the ionicity of the bonds and, as a result, their lengths are influenced by the following secondary effects: (a) An increase in the oxidation state of the central atom generally increases its effective electronegativity and results in increased covalency and, hence, shorter bonds. It must be kept in mind, however, that the addition of two fluorine ligands results in a considerably stronger electron density withdrawal from the central atom than that caused by the addition of one doubly bonded oxygen ligand. Thus, for extremely electronegative central atoms, such as chlorine in ClF_2^+ or ClF_4^-, the addition of an oxygen ligand may even result in the reverse effect, i.e. the release of electron density to the central atom.[62,63] (b) In the case of coordination number (CN) seven, steric crowding and, hence, repulsion effects also become important. The increased congestion in the equatorial planes of IF_7 and IOF_6^-, for example, results in increased mutual repulsion and increased lengths of the equatorial bonds. Thus, the nearest-neighbor $F_{eq}\cdots F_{eq}$ contacts in the IOF_6^- anion at −93 °C are 2.090(16)–2.362(12) Å and are significantly less than twice the nominal van der Waals radius for fluorine, i.e., 2.70–2.80 Å,[44,45] while in hexacoordinated IF_5[38] the nearest neighbor $F_{eq}\cdots F_{eq}$ contacts are 2.571 Å and are still at the limit of the sum of the fluorine van der Waals radii. Similarly, the increased repulsion from the sterically active, free valence electron pair on iodine in heptacoordinated IF_6^- causes an elongation of the three neighboring I–F bonds.[61] (c) A formal negative charge, as found in an anion, enhances the $F^{\delta-}$–$I^{\delta+}$ bond polarity and hence the ionicity of a bond and, thereby, increases the bond lengths.[62]

The combination of these effects can explain the features of the compounds shown in Figure 6. For IOF_6^-, the relative length of equatorial I–F bonds can be explained by semi-ionic, multicenter bonding, which is enhanced by the formal negative charge and the repulsion effects caused by the steric crowding in the equatorial plane, while the lengthening of the I–O bond is attributed mainly to the formal negative charge and the repulsion effects. There is one piece of data in Figure 6, however, which does not fit the overall picture. This is the axial I–F bond length in IOF_5. The published[38] value of 1.863 Å appears too long and, based on the fact that the axial IF stretching force constant in IOF_5 is larger than the equatorial one[64] and by analogy with the isoelectronic $TeOF_5^-$ anion ($Te–F_{ax}$ = 1.854 Å, $Te–F_{eq}$ = 1.853 Å),[65] the axial bond distance in IOF_5 should be similar to or shorter than the equatorial ones. A cursory examination[66] of the experimental data[38,64,67–69] available for IOF_5 revealed that these bond distances are not well-determined and are very sensitive to the choice of the $O–I–F_{eq}$ bond angle. Thus, a decreasing angle lengthens the I–O and shortens the $I–F_{ax}$ bond. Furthermore, a lengthening of the $I–F_{eq}$ bond distance results in a shortening of the $I–F_{ax}$ bond distance. Obviously, additional experimental data are required for a more precise structure determination of IOF_5.

Conclusions. The IOF_6^- anion provides unique information on the nature of heptacoordinated molecules. The high degree of fluxionality, which is normally encountered for free heptacoordinated molecules, is absent. Dynamic puckering of the equatorial ligand plane is frozen out by crystal forces, and axial–equatorial ligand exchange is precluded by the incorporation of the more repulsive, axial oxygen ligand. It is shown that the statically puckered, equatorial fluorine plane exhibits C_s symmetry in the crystal. Furthermore, it is demonstrated by ab initio calculations and the crystal structure of XeF_5^- that the lowest energy structures of these molecules are pentagonal bipyramids with coplanar equatorial ligands. This coplanarity is explained by a bonding scheme involving delocalized, planar p_z^2–p_z^2 hybrid orbitals of the central atom for the formation of a semi-ionic, 6-center 10-electron system for the five $I–F_{eq}$ bonds which also accounts for their increased lengths. The degree of puckering of the equatorial ligand plane increases with increasing mutual repulsion of the equatorial ligands and, therefore, is temperature dependent as demonstrated for IOF_6^-.

Acknowledgment. The work at Rocketdyne was financially supported by the U.S. Air Force Phillips Laboratory and the U.S. Army Research Office, that at McMaster University by the U.S. Air Force Phillips Laboratory and the Natural Sciences and Engineering Research Council of Canada, and that at Freie Universität Berlin by the Deutsche Forschungsgemeinschaft. We also thank Professor Neil Bartlett, Dr. A. J. Arduengo, Dr. C. J. Schack and Mr. R. D. Wilson for helpful discussions and Professor S. Kukolich for the calculations on the structure of IOF_5.

Supplementary Material Available: A structure determination summary (Table S1), final atomic coordinates, equivalent isotropic displacement coefficients, and site occupancy factors (Table S4), anisotropic displacement coefficients (Table S5), and symmetry coordinates (Table S6) (6 pages); calculated and observed structure factor amplitudes (Tables S2 and S3) (16 pages). Ordering information is given on any current masthead page.

(62) Christe, K. O.; Schack, C. J. *Adv. Inorg. Chem. Radiochem.* **1976**, *18*, 331. Christe, K. O. *XXIVth Int. Congr. Pure Appl. Chem.* **1974**, *4*, 115.
(63) Christe, K. O.; Curtis, E. C. *Inorg. Chem.* **1972**, *11*, 2209.
(64) Smith, D. F.; Begun, G. M. *J. Chem. Phys.* **1965**, *43*, 2001. Holloway, J. H.; Selig, H.; Claassen, H. H. *J. Chem. Phys.* **1971**, *54*, 4305.
(65) Miller, P. K.; Abney, K. D.; Rappé, A. K.; Anderson, O. P.; Strauss, S. H. *Inorg. Chem.* **1988**, *27*, 2255.
(66) Kukolich, S. G., private communication of unpublished results.
(67) Brier, P. N. *J. Mol. Spectrosc.* **1987**, *125*, 233.
(68) Brier, P. N.; Winrow, M. J. *J. Mol. Spectrosc.* **1984**, *107*, 21.
(69) Pierce, S. B.; Cornwell, C. D. *J. Chem. Phys.* **1967**, *47*, 1731.